Development 137, 4221-4227 (2010) doi:10.1242/dev.057117

Non-cell-autonomously coordinated organ size regulation in leaf development

Kensuke Kawade[1], Gorou Horiguchi[2,*] and Hirokazu Tsukaya[1,3]

SUMMARY

The way in which the number and size of cells in an organ are determined poses a central challenge in our understanding of organ size control. Compensation is an unresolved phenomenon, whereby a decrease in cell proliferation below some threshold level triggers enhanced postmitotic cell expansion in leaf primordia. It suggests an interaction between these cellular processes during organogenesis and provides clues relevant to an understanding of organ size regulation. Although much attention has been given to compensation, it remains unclear how the cellular processes are coordinated. Here, we used a loss-of-function mutation in the transcriptional coactivator gene *ANGUSTIFOLIA3* (*AN3*), which causes typical compensation in *Arabidopsis thaliana*. We established Cre/*lox* systems to generate leaves chimeric for AN3 expression and investigated whether compensation occurs in a cell-autonomous or non-cell-autonomous manner. We found that *an3*-dependent compensation is a non-cell-autonomous process, and that *an3* cells seem to generate and transmit an intercellular signal that enhances postmitotic cell expansion. The range of signalling was restricted to within one-half of a leaf partitioned by the midrib. Additionally, we also demonstrated that overexpression of the cyclin-dependent kinase inhibitor gene *KIP-RELATED PROTEIN2* resulted in cell-autonomous compensation. Together, our results revealed two previously unknown pathways that coordinate cell proliferation and postmitotic cell expansion for organ size control in plants.

KEY WORDS: *AN3*, Compensation, Leaf chimera, *KRP2*, Organ size, *Arabidopsis thaliana*

INTRODUCTION

Organ size is determined by the number and size of constituent cells and is genetically regulated in a highly reproducible manner. Cell proliferation and postmitotic cell expansion are hence coordinated, yet the mechanisms behind these processes remain poorly understood.

In plants, spatiotemporal regulation of cell proliferation and postmitotic cell expansion is seen during leaf development. Cell proliferation is active throughout the developing leaf primordium, but it ceases from the distal to proximal region (Donnelly et al., 1999; Ichihashi et al., 2010; Kazama et al., 2010; Nath et al., 2003; White, 2006). There is a proximal-distal gradient of cell proliferation activity, whereby proliferation in the proximal region and postmitotic expansion in the distal region occur simultaneously in the same leaf primordium. During leaf development, a defect in cell proliferation often triggers enhanced cell expansion, a phenomenon that was first described nearly half a century ago in γ-irradiated wheat (Haber, 1962). More recently, similar phenomena have been reported using various mutants and transgenic strains of *Arabidopsis thaliana* (hereafter *Arabidopsis*) (Micol, 2009; Tsukaya, 2008). These phenomena have been collectively termed 'compensation' (Beemster et al., 2003; Tsukaya, 2002; Tsukaya, 2008). Compensation seems to occur only in determinate organs, such as leaves (Ferjani et al., 2007). It suggests an interaction of cell proliferation and expansion, and provides clues that are relevant to an understanding of organ size control (Tsukaya, 2008).

The loss-of-function mutant *angustifolia3* (*an3*) and the overexpressor of the cyclin-dependent kinase inhibitor gene *KIP-RELATED PROTEIN2* (*KRP2* o/x) show features typical of compensation (De Veylder et al., 2001; Ferjani et al., 2007; Hemerly et al., 1995; Horiguchi et al., 2005). In the leaves of *an3* and *KRP2* o/x, cell number is decreased by more than 70% and 90% and cell size is increased by 50% and 100%, respectively, as compared with the wild type (WT) (De Veylder et al., 2001; Ferjani et al., 2007; Horiguchi et al., 2005). *AN3* (which is also known as *GRF-INTERACTING FACTOR1*) encodes a transcriptional coactivator (Kim and Kende, 2004). KRP2, which is identical to *Arabidopsis* Cdc-2a-interacting protein ICK2, binds and inhibits A-type cyclin-dependent kinase, thereby restricting cell cycle progression (De Veylder et al., 2001; Lui et al., 2000; Verkest et al., 2005).

Studies on *an3*-dependent compensation (Ferjani et al., 2007; Fujikura et al., 2007a; Fujikura et al., 2009) have indicated that the size of mitotic cells is normal but that enhanced expansion occurs in postmitotic cells in the *an3* mutant; furthermore, there is a threshold decrease in cell number or cell proliferation activity that induces compensation. Moreover, *an3*-dependent compensation is completely suppressed in a group of *extra-small sisters* (*xs*) mutants that are specifically defective in postmitotic cell expansion. These data suggest that *an3*-dependent compensation is not simply the result of a defect in cell proliferation; it probably involves an interaction between cell proliferation and postmitotic cell expansion.

We consider that compensation occurs in three successive steps. The induction step involves a defect in cell proliferation. The intermediary step links cell proliferation with postmitotic cell expansion through an unknown signal. This signal regulates the

[1]Department of Biological Sciences, Graduate School of Science, The University of Tokyo, 7-3-1 Hongo, Bunkyo-ku, Tokyo 113-0033, Japan. [2]Department of Life Science, College of Science, Rikkyo University, 3-34-1 Nishi-Ikebukuro, Toshima-ku, Tokyo 171-8501, Japan. [3]National Institute for Basic Biology, 38 Nishigo-Naka, Myodaiji-cho, Okazaki, Aichi 444-8585, Japan.

*Author for correspondence (ghori@rikkyo.ac.jp)

Accepted 15 October 2010

response step, which results in the intense expansion of postmitotic cells. In this study, we focused on the intermediary step because how the defect in cell proliferation is linked with postmitotic cell expansion is totally unknown. We assumed a cell-autonomous or non-cell-autonomous mode of action in the intermediary step (Fujikura et al., 2007b). Here, we induced leaf chimeras for AN3 or KRP2 expression to investigate the mechanism of compensation. Based on our results, we discuss the mechanisms that coordinate cell proliferation and postmitotic cell expansion for organ size control.

MATERIALS AND METHODS

Plant materials and growth conditions

The WT accession used in this study was Columbia-0. Plants were grown on rock wool at 22°C under a 16 hours light/8 hours dark cycle. Light intensity, at ~50 μmol m^{-2} s^{-1}, was provided by white fluorescent lamps. Plants were watered daily with 0.5 g/l Hyponex solution (Hyponex). For in vitro culture, surface-sterilised seeds were sown on Murashige and Skoog medium (Murashige and Skoog, 1962) containing Gamborg's B5 vitamins (Gamborg et al., 1968), 3% (w/v) sucrose and 0.5% (w/v) gellan gum (pH 5.8).

Transgenic plants for clonal analysis

Vectors for clonal analysis were constructed as described below. A chimeric gene encoding AN3 tagged with triple green fluorescent protein (3xGFP) at its C-terminus was produced as follows. *AN3* cDNA that lacks the termination codon and is flanked by an *Xho*I and a *Sal*I site was amplified by PCR using oligonucleotides 5′-CTCGAGCAAAAG-AAATGGCTGGTTACTACCCCAG-3′ and 5′-GTCGACATTCCCAT-CATCTGATGATTTC-3′ and cloned into the pGEM T-Easy vector (Promega). Then, an internal *Xho*I site of the *AN3* cDNA was replaced by a synonymous mutation using PCR-mediated site-directed mutagenesis with oligonucleotides 5′-TGGAATGAGCTCAAGCAGCGGAGGA-3′ and 5′-TCCTCCGCTGCTTGAGCTCATTCCA-3′. The resultant cDNA was excised by *Xho*I and *Sal*I and inserted into the *Xho*I site of pGEM 3xGFP that contained 3xGFP with the termination codon (Y. Ichihashi, G.H., T. Takahashi and H.T., unpublished) to yield pGEM AN3-3xGFP.

A chimeric gene encoding 3xGFP that was C-terminally fused with KRP2 (3xGFP-KRP2) was generated as follows. The *KRP2* cDNA flanked by an *Xho*I and a *Sal*I site was amplified by PCR using oligonucleotides 5′-CTCGAGATATGGCGGCGGTTAGG-3′ and 5′-GTCGACTGGAT-TCAATTTAACCCACT-3′ and cloned into the pGEM T-Easy vector. A *3xGFP* gene without the termination codon was prepared by amplifying *GFP* cDNA using oligonucleotides 5′-CTCGAGGGAGGCGGTGGAG-GCATG-3′ and 5′-GTCGACCTTGTACAGCTCGTCCATGC-3′ and pH35WG (G.H. and H.T., unpublished) as a template. The resultant *GFP* cDNA was cloned into the pGEM T-Easy vector (pGEM GFP). The *GFP* cDNA fragment was excised by *Xho*I and *Sal*I and re-inserted into the *Xho*I site of pGEM GFP. This step was repeated once more to yield pGEM 3xGFP(–) that contained termination codon-less 3xGFP. The *KRP2* cDNA was excised by *Xho*I and *Sal*I and inserted into the *Sal*I site of pGEM 3xGFP(–) to yield pGEM 3xGFP-KRP2.

We previously prepared pGEM LLG containing a cauliflower mosaic virus 35S terminator flanked by two *lox* sites and a *GUS* cDNA behind it, and pGEM LGL containing a GUS-35S terminator cassette between two *lox* sites (Y. Ichihashi, G.H., T. Takahashi and H.T., unpublished). pGEM AN3-3xGFP and pGEM 3xGFP-KRP2 were excised by *Xho*I and *Sal*I and inserted into the *Xho*I site of pGEM LLG or the *Sal*I site of pGEM LGL to yield pGEM L-AN3-3xGFP-L-G, pGEM L-3xGFP-KRP2-L-G, pGEM LGL-AN3-3xGFP and pGEM LGL-3xGFP-KRP2. Finally, these *lox* cassettes were excised by *Xba*I and *Sac*I and inserted into the same restriction sites of binary vector pSMAB704 to generate expression constructs. These vectors were used to transform the *an3-4* mutant or WT for *AN3* or *KRP2* clonal analyses, respectively.

HSP::Cre lines were provided by Prof. T. Takahashi (Okayama University, Japan). *HSP::Cre* lines containing the *an3-4* mutation (*an3-4/HSP::Cre*) were established by crossing *HSP::Cre* with *an3-4*. Establishment of transgenic lines has been described previously (Clough and Bent, 1998; Fujikura et al., 2009). At least two independent single-insertion lines were established for each construct.

Generation of leaves chimeric for AN3 and KRP2 expression

The genetic strategy for clonal analysis by Cre/*lox*-mediated recombination was based on previously described methods (Serralbo et al., 2006; Sieburth et al., 1998). Transgenic lines harbouring *35S::lox::GUS::lox::AN3-GFP-GFP-GFP* (*AN3-act*) or *35S::lox::AN3-GFP-GFP-GFP::lox::GUS* (*AN3-del*) in an *an3-4* background were crossed with *an3-4/HSP::Cre*. Transgenic lines harbouring *35S::lox::GUS::lox::GFP-GFP-GFP-KRP2* (*KRP2-act*) or *35S::lox::GFP-GFP-GFP-KRP2::lox::GUS* (*KRP2-del*) in a WT background were crossed with *HSP::Cre*. F1 progeny, with both constructs (referred to as *an3-4/HSP::Cre; AN3-act*, *an3-4/HSP::Cre; AN3-del*, *HSP::Cre; KRP2-act* and *HSP::Cre; KRP2-del* in this study) were used for clonal analyses. For generation of sectorial or spotted leaves chimeric for AN3 expression, heat shock (HS) at 37°C was carried out for 60 minutes with 1- or 4-day-old seedlings, respectively. For generation of sectorial or spotted leaves chimeric for KRP2 expression, HS at 37°C was carried out for 90 minutes with 2- or 6-day-old seedlings, respectively.

Microscopy

For morphological and cellular analyses, the first leaves dissected from 21-day-old plants were briefly centrifuged before observation, as described previously (Horiguchi et al., 2006). Whole leaves were observed under a stereoscopic microscope (MZ16a; Leica Microsystems) and palisade cells in the subepidermal layer were examined using a Nomarski differential interference contrast microscope (DMRX/E; Leica Microsystems). The average leaf area (n=8 leaves) and cell size (n=160 cells from at least eight leaves) were measured according to Fujikura et al. (Fujikura et al., 2009). The total cell number of palisade cells in the subepidermal layer was estimated according to Horiguchi et al. (Horiguchi et al., 2005). Excitation of GFP was performed by standard methods.

RESULTS

Strategy for clonal analysis using *AN3* chimeric leaves

We established heat shock (HS)-dependent *AN3* activation and deletion systems (Fig. 1) by applying a Cre/*lox*-mediated recombination mechanism (Y. Ichihashi, G.H., T. Takahashi and H.T., unpublished). In these systems, expression of AN3 tagged with triple green fluorescent protein (3xGFP) was either activated (Fig. 1A) or repressed (Fig. 1B) in the *an3-4* background upon HS. Neither HS treatment nor expression of *3xGFP* or β-*glucuronidase* (*GUS*) affected normal leaf development (see Fig. S1 in the supplementary material). We could induce HS-dependent recombination in cells of entire primordia (see Fig. S2 in the supplementary material) or in parts of leaf primordia (see below) by optimising the HS conditions. We confirmed that AN3-3xGFP had a comparable cell proliferation-promoting activity to native AN3, and that our *AN3* activation and deletion systems were properly established for the analyses described below (see Figs S2 and S3 in the supplementary material).

an3-dependent compensation acts in a non-cell-autonomous manner

Chimeric leaves were generated in *an3-4* harbouring single *HSP::Cre* and *35S::lox::GUS::lox::AN3-3xGFP* (*AN3-act*) copies (Fig. 1A) (referred to as *an3-4/HSP::Cre; AN3-act*) by HS at 37°C for 60 minutes at 1 day after sowing (DAS). We selected a particular type of leaf chimera that contained a longitudinal *AN3* overexpressor (o/x) sector (Fig. 2A). These plants had asymmetric leaf blades because of the effect of this sectorial expression of AN3-3xGFP (Fig. 2A). We could clearly observe the boundary between GFP-positive

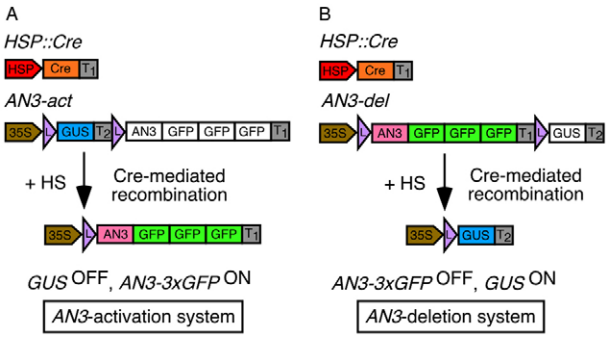

Fig. 1. Experimental design for *AN3* clonal analysis. Structure of the DNA constructs for the *AN3* (**A**) activation and (**B**) deletion systems. Expression of *Cre* was under the control of the *HSP18.2* promoter (HSP) (Takahashi and Komeda, 1989). β-*glucuronidase* (GUS) or *AN3-3xGFP* (AN3) was placed downstream of a 35S promoter (35S) between two Cre-targeting *lox* sites (L) in *AN3-act* (A) or *AN3-del* (B) vectors, respectively. *AN3* expression was induced or suppressed in transgenic *Arabidopsis* plants harbouring *AN3-act* or *AN3-del* with *an3-4/HSP::Cre* after heat shock (HS)-dependent recombination by Cre recombinase. T1 and T2 represent the nopaline synthase and 35S terminators, respectively. Coloured rectangles depict active genes.

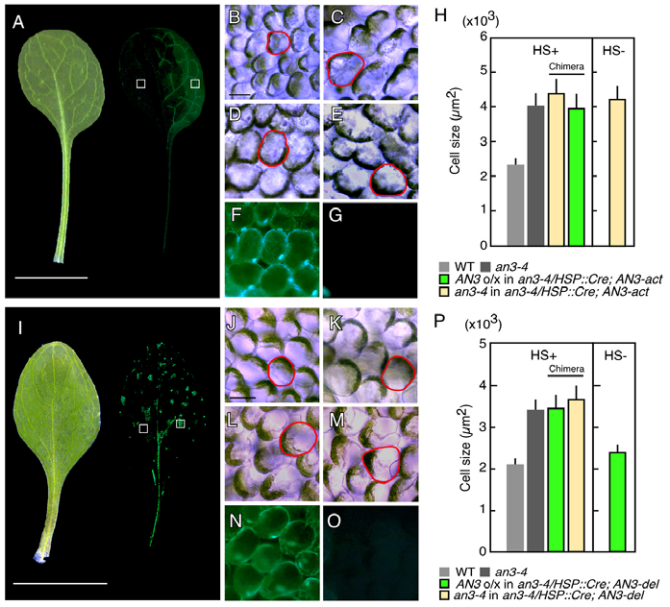

Fig. 2. Non-cell-autonomous regulation of *an3*-dependent compensation. (**A**) Bright-field (left) and GFP fluorescence (right) images of a chimeric *Arabidopsis* leaf containing a longitudinal *AN3* overexpressor (o/x) sector induced by the *AN3* activation system (see Fig. 1A). Squares indicate the region where the size of palisade cells was measured. (**B-G**) Bright-field (B-E) and GFP fluorescence (F,G) images of palisade cells in the WT (B), *an3-4* (C), and in leaf chimera with *AN3* o/x (D,F) and *an3-4* (E,G) genotypes observed from a paradermal view. Typically sized cells of each genotype are outlined in red (B-E). (**H**) The size of the palisade cells in the WT, *an3-4*, and in leaf chimera with *AN3* o/x and *an3-4* genotypes, with a non-HS *an3-4/HSP::Cre; AN3-act* leaf shown as a control (HS–). The mean ± s.d. from eight individual leaves is indicated. (**I**) Bright-field (left) and GFP fluorescence (right) images of chimeric leaves in which small cell clusters with the *AN3* o/x genotype were randomly distributed in an *an3-4* background induced by the *AN3* deletion system (see Fig. 1B). Squares indicate the region where the size of the palisade cells was measured. (**J-O**) Bright-field (J-M) and GFP fluorescence (N,O) images of palisade cells in the WT (J), *an3-4* (K), and in leaf chimera with *AN3* o/x (L,N) and *an3-4* (M,O) genotypes observed from a paradermal view. Typically sized cells of each genotype are outlined in red (J-M). (**P**) The size of the palisade cells in the WT, *an3-4*, and in leaf chimera with *AN3* o/x and *an3-4* genotypes, with a non-HS *an3-4/HSP::Cre; AN3-del* leaf shown as a control (HS–). The mean ± s.d. from eight individual leaves is indicated. Scale bars: 5 mm in A,I; 50 μm in B,J.

and GFP-negative cells, suggesting that intercellular AN3-3xGFP movement was unlikely (see Fig. S4 in the supplementary material). Following HS, the *AN3* o/x genotype extended through various cell layers (including epidermis, palisade tissue and/or spongy tissues; data not shown). We measured cell size in the regions where the cells in all layers had either the *AN3* o/x or the *an3-4* genotype (Fig. 2A, squares). We excluded the sector boundaries from our analyses because in these regions we found aberrantly small cells (see Fig. S4 in the supplementary material). In these leaf chimeras, we found that *AN3* o/x cells showed full compensation that was comparable to *an3-4* cells in the leaf chimera of the same line and also in non-chimeric *an3-4* leaves (Fig. 2B-H). This result suggests that *an3*-dependent compensation is a non-cell-autonomous process, and that *an3-4* cells have a dominant role in intercellular cell size regulation in these chimeric leaves.

The shape of the clones in our leaf chimeras might have affected cell expansion physically. Additionally, cell size might to be predetermined depending on the genotype of the leaf primordia before HS. In these cases, the presence of this intercellular signalling can be questioned. Thus, we investigated chimeric leaves containing clones of another shape induced by an *AN3* deletion system in which *AN3-3xGFP* was removed by HS (Fig. 1B). We determined the HS conditions required for induction of chimeric leaves in which small clusters of *AN3* o/x cells were randomly distributed amongst a background of those with the *an3-4* genotype (Fig. 2I). Chimeric leaves were generated in the *an3-4* harbouring single *HSP::Cre* and *35S::lox::AN3-3xGFP::lox::GUS* (*AN3-del*) copies (referred to as *an3-4/HSP::Cre; AN3-del*) by HS at 37°C for 90 minutes at 4 DAS. We found that even *AN3* o/x cells in the chimeric leaves showed full compensation (Fig. 2J-P). By contrast, compensation was absent in non-HS *AN3* o/x cells in the same line (Fig. 2P). This result demonstrated that final cell size was not predetermined in very early leaf primordia. Furthermore, the shapes of the clones had no effect on cell size. These data indicate that *an3*-dependent compensation is induced non-cell-autonomously.

Intercellular signalling in *an3*-dependent compensation is restricted to within one-half of a leaf partitioned by a midrib

Most of our leaf chimeras contained a longitudinal *AN3* o/x sector; in some cases, the *AN3* o/x cells were separated from the *an3-4* cells by a midrib of *AN3* o/x cells (Fig. 3A). The sizes of the *AN3* o/x and *an3-4* cells in these chimeric leaves were similar to those of the WT and *an3-4* mutant, respectively, regardless of the distance from the sector boundaries (Fig. 3B,C). This finding indicates that intercellular signalling in *an3*-dependent compensation in these chimeric leaves was restricted to within one-half of a leaf blade partitioned by the midrib. In agreement with this idea, *AN3* o/x cells that co-existed with the *an3-4* cells on one side of the midrib showed compensation, whereas *AN3* o/x cells on the other side of the midrib without *an3-4* cells did not (see Fig. S5 in the supplementary material).

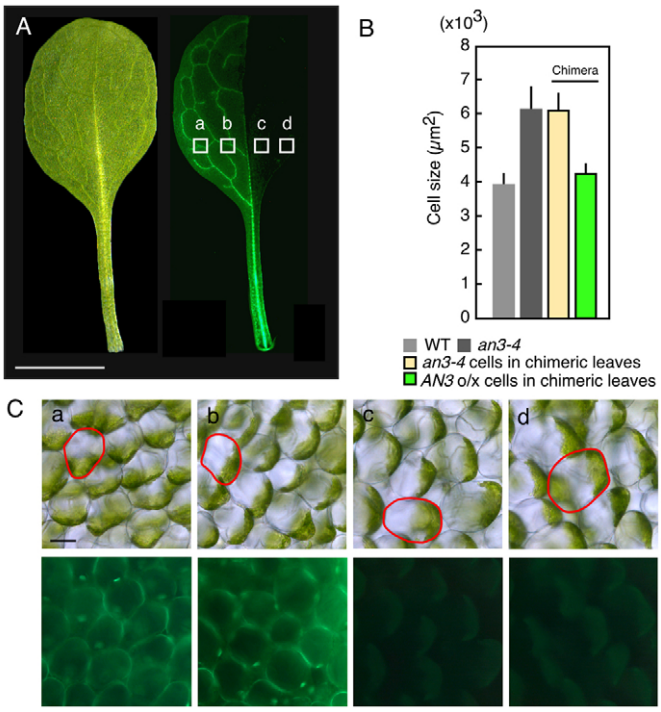

Fig. 3. Characterisation of intercellular signalling in *an3*-dependent compensation. (**A**) Bright-field (left) and GFP fluorescence (right) images of a chimeric *Arabidopsis* leaf in which *AN3* o/x and *an3-4* clones were separated by the midrib. The chimeric leaf was generated in the *an3-4/HSP::Cre; AN3-act* line by HS at 37°C for 60 minutes at 1 day after sowing (DAS). (**B**) The sizes of the palisade cells in the *AN3* o/x and *an3-4* regions of the chimeric leaves, with WT and *an3-4* leaves shown as a control. The mean ± s.d. from eight individual leaves is indicated. (**C**) Bright-field (upper row) and GFP fluorescence (lower row) images of palisade cells from regions (a-d) of the chimeric leaves indicated in A.

Cell-autonomous action of compensation induced by *KRP2* overexpression

The results reported here describe a non-cell-autonomous mechanism that coordinates cell proliferation and postmitotic cell expansion during leaf development. To determine whether this is a common property of the coordination mechanism, we investigated whether compensation induced by *KRP2* overexpression is mediated in a cell-autonomous or non-cell-autonomous manner using a *KRP2* deletion system (Fig. 4A; see Fig. S6 in the supplementary material). The experimental design for *KRP2* clonal analysis was similar to that described for *AN3*.

We induced leaves chimeric for KRP2 expression by HS treatment (37°C for 60 minutes at 6 DAS) using the *KRP2* deletion system (Fig. 4A). The leaf morphology of the chimera was similar to that of the constitutive *KRP2* o/x (Fig. 4B; see Fig. S6 in the supplementary material), but there was a co-existence of GFP-positive (*KRP2* o/x) and GFP-negative (WT) cells (Fig. 4C,D). We found that the sizes of *KRP2* o/x and WT cells in these chimeric leaves were similar to those of the constitutive *KRP2* o/x line and the WT, respectively (Fig. 4E). These data indicated that compensation induced by *KRP2* overexpression is regulated in a cell-autonomous manner.

We analysed chimeric leaves induced by a *KRP2* activation system in order to account for the effect of clone distribution on cell size (Fig. 4F). We induced chimeric leaves containing a *KRP2* o/x sector by HS treatment (37°C for 60 minutes at 2 DAS) of the transgenic line harbouring single *HSP::Cre* and *35S::lox::GUS::lox::3xGFP-KRP2* (*KRP2-act*) copies in a WT background (referred to as *HSP::Cre; KRP2-act*) (Fig. 4G,H). The *KRP2* o/x cells showed compensation, whereas the WT cells did not (Fig. 4I-K). In contrast to *AN3* leaf chimeras, enhanced cell expansion was consistently observed in *KRP2* o/x cells, even along the sector boundaries (Fig. 4I-K). These results demonstrated that compensation induced by *KRP2* overexpression occurred cell-autonomously.

KRP2 has no direct function in enhanced cell expansion in postmitotic cells

Compensation in *KRP2* o/x was found to be regulated in a cell-autonomous manner, in contrast to that described for *an3*. This raises the possibility that KRP2 might have a direct effect on the enhancement of cell expansion in postmitotic cells. Studies have reported that *KRP2* is expressed more abundantly in expanding and endoreduplicating tissue than in the actively proliferating tissues in the WT (Ormenese et al., 2004; Verkest et al., 2005). Thus, we investigated the effect of *KRP2* overexpression in postmitotic cells. We analysed the *HSP::Cre; KRP2-act* line in which *KRP2* overexpression was induced at 4, 7 and 10 DAS by HS at 37°C for 90 minutes. In these plants, GFP signal was detected in most cells in the first leaves (data not shown). Our previous data indicated that cell proliferation terminates at ~11 DAS in the first leaves of the WT (Ferjani et al., 2007). If KRP2 directly enhances the expansion of postmitotic cells, cells in this line should exhibit compensation in response to HS even after exiting the mitotic cell cycle. When *KRP2* overexpression was induced at 4 DAS, it affected leaf morphology (Fig. 5A), and compensation was observed throughout the leaves (Fig. 5B). Induction of *KRP2* overexpression at 7 DAS resulted in induction of compensation in the proximal region of the first leaves, but the size of the cells in the distal region was similar to that of non-HS cells of the same line (Fig. 5B). These results might be explained by a proximal-distal gradient of cell proliferation activity because at 7 DAS, postmitotic cells were observed in the distal region of the first leaves, whereas actively proliferating cells were still seen proximally (Ferjani et al., 2007). Importantly, no enhanced cell expansion was observed when *KRP2* overexpression was induced at 10 DAS (Fig. 5B). These data demonstrate that to induce compensation *KRP2* must be overexpressed in cells at the stage of active proliferation.

an3 has an additive effect on cell proliferation in *KRP2* o/x

To investigate the genetic relationship between *an3* and *KRP2* o/x in leaf development, we analysed the leaf phenotypes of the *an3* mutant overexpressing *KRP2*. The *an3-4* mutation decreased the cell number in the first leaves by 73%, as compared with the WT. The first leaves of *an3 KRP2* o/x showed a similar decrease in cell number (70%), compared with *KRP2* o/x (Fig. 6A). This result indicated that the *an3-4* mutation had an additive effect on cell proliferation in *KRP2* o/x. The size of the cells in *an3 KRP2* o/x was increased, compared with those in *an3* and *KRP2* o/x (Fig. 6B,D-G), indicating that enhanced cell expansion in *an3* is further promoted by compensation induced by *KRP2* overexpression. The leaf area of *an3 KRP2* o/x was decreased compared with that of WT, *an3-4* and *KRP2* o/x, owing to the decrease in the number of cells (Fig. 6C,H).

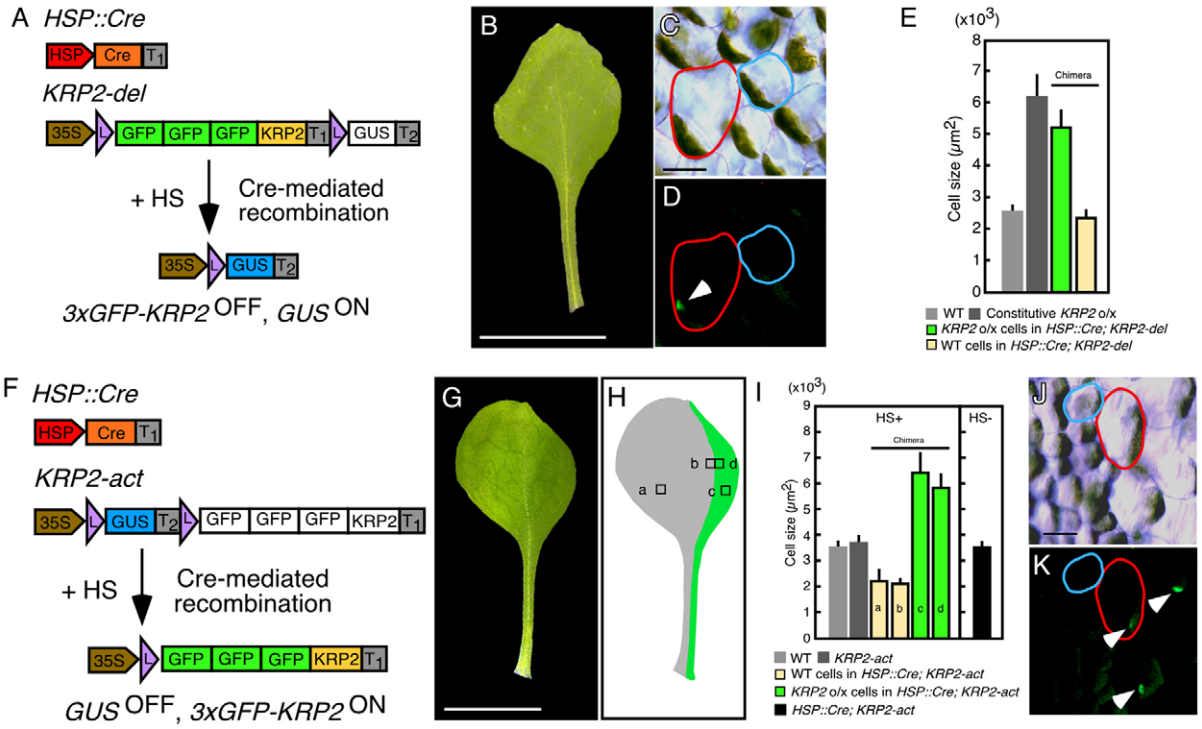

Fig. 4. Cell-autonomous regulation of compensation in *KRP2* o/x. (**A**) Structure of the DNA construct for the *KRP2* deletion system. HS treatment induced the expression of Cre recombinase, which removed the *3xGFP-KRP2* region. As a consequence of recombination, WT cells were generated and are visually distinguishable from *KRP2* o/x cells by the loss of the GFP signal. (**B**) A chimeric *Arabidopsis* leaf in which small cell clusters with the *KRP2* o/x genotype were randomly distributed in a WT background induced by the *KRP2* deletion system. (**C**,**D**) Bright-field (C) and GFP fluorescence (D) images of palisade cells in the chimeric leaves observed from a paradermal view. GFP fluorescence (green) marks the nuclei of *KRP2*-overexpressing cells (arrowhead). Typically sized *KRP2* o/x and WT cells are outlined in red and blue, respectively. (**E**) The size of the palisade cells in the WT, constitutive *KRP2* o/x, and in leaf chimera with *KRP2* o/x and WT genotypes. The mean ± s.d. from eight individual leaves is indicated. (**F**) Structure of the DNA construct for the *KRP2* activation system. HS treatment induced the expression of Cre recombinase, which removed the *GUS* region. As a result of recombination, *KRP2* o/x cells were generated in which the nucleus is marked with a GFP signal. (**G**,**H**) A chimeric leaf containing a longitudinal *KRP2* o/x sector induced by the *KRP2* activation system (G). WT (grey) and *KRP2* o/x (green) clones are distributed as illustrated (H). (**I**) The size of the palisade cells in the WT, *KRP2-act* homozygote, and in leaf chimera with *KRP2* o/x and WT genotypes. The regions where cell size was measured (a-d) are indicated in H. The size of the palisade cells in non-HS *HSP::Cre; KRP2-act* leaves is shown as a control. The mean ± s.d. from eight individual leaves is indicated. (**J**,**K**) Bright-field (J) and GFP fluorescence (K) images of palisade cells at the boundary between the WT and *KRP2* o/x sectors in chimeric leaves, as observed from a paradermal view. GFP fluorescence marks the nucleus of *KRP2*-overexpressing cells (arrowheads). Typically sized *KRP2* o/x and WT cells are outlined in red and blue, respectively. Scale bars: 5 mm in B,G; 50 μm in C,J.

DISCUSSION

In this study, we demonstrated that two qualitatively different modes (i.e. non-cell-autonomous and cell-autonomous modes in *an3* and *KRP2* o/x, respectively) are involved in the coordination of cell proliferation and postmitotic cell expansion in leaves. Genetic analysis of *an3-4 KRP2* o/x indicated that the *an3* mutation and *KRP2* overexpression trigger compensation through different mechanisms.

Our findings from clone analysis provide important insights into the coordination mechanisms that operate between cell proliferation and postmitotic cell expansion. We showed that even *AN3* o/x cells exhibited full compensation when they co-existed with *an3-4* cells in a chimeric leaf. This result suggests that an intercellular signalling molecule (‘factor X’) that enhances postmitotic cell expansion is abundantly produced in the *an3-4* cells and transmitted from cell to cell. Furthermore, we observed a distinct type of intercellular signalling from a specific type of chimera: when *AN3* expression was induced in one-half of a chimeric leaf, *AN3* o/x cells did not show compensation, although *an3-4* cells on the other side did. This suggests that the intercellular signalling mechanism involved in *an3*-dependent compensation is limited to within one-half of a leaf. The discovery of subdivided compartments in the leaf primordium will provide novel insight into the intercellular mechanisms that are responsible for the coordination of cellular processes during leaf development.

A positive correlation is often seen between cell size and the level of endoreduplication (e.g. Melaragno et al., 1993); however, the ploidy level of leaf cells in the *an3* mutant is relatively normal (Fujikura et al., 2007a). This suggests that factor X modulates an endopolyploidy-independent cell expansion pathway. Previous analyses have shown that enhancement of cell expansion in the *an3* mutant is due to an increase in the rate, not the period, of postmitotic cell enlargement (Ferjani et al., 2007). In addition, a subset of *XS* genes involved in normal cell expansion has a role in the *an3*-dependent compensation. The *xs1*, *xs2*, *xs4* and *xs5* mutant lines show decreased cell size, but normal cell numbers, in leaves. In *xs an3* double mutants, *an3*-dependent compensation is fully suppressed (Fujikura et al., 2007a). Thus, factor X seems to

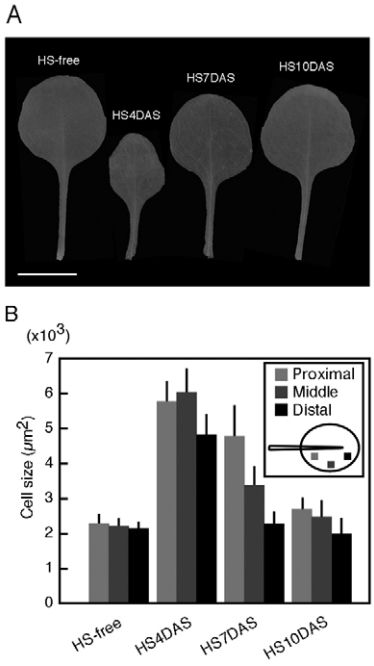

Fig. 5. KRP2 has no direct function in enhanced cell expansion in postmitotic cells. (**A**) The first leaves of an HS *HSP::Cre; KRP2-act Arabidopsis* plant, in which *KRP2* overexpression was induced at 4, 7 and 10 DAS. A leaf from a non-HS plant of the same line is shown as a control. Scale bar: 5 mm. (**B**) The size of palisade cells from non-HS and HS *HSP::Cre; KRP2-act* leaves in which *KRP2* overexpression was induced at 4, 7 and 10 DAS. Cell size was measured at the proximal, middle and distal regions of the first leaves (see key). The mean ± s.d. from eight individual leaves is indicated.

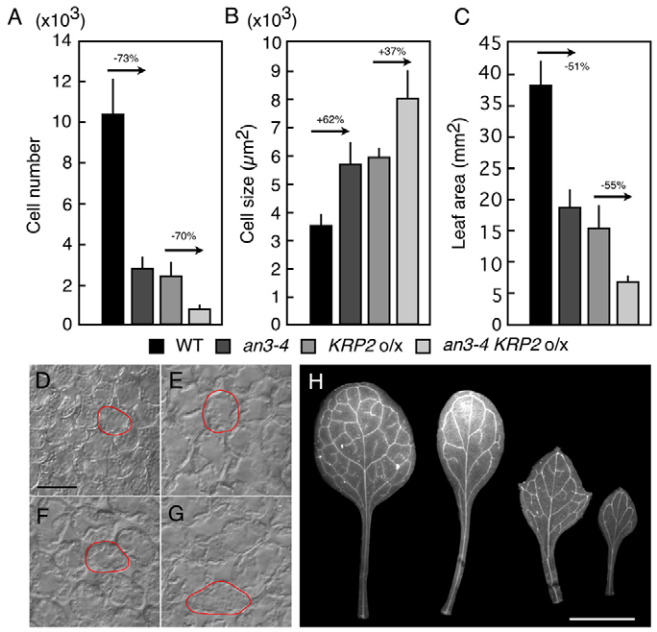

Fig. 6. Double-mutant analysis of cell and leaf morphology. (**A-C**) Number (A) and size (B) of palisade cells in the subepidermal layer and leaf blade area (C) of the first leaves of WT, *an3-4*, *KRP2* o/x and *an3-4 KRP2* o/x. The mean ± s.d. from eight individual leaves is indicated. Arrows indicate the difference between adjacent bars. (**D-G**) Palisade cells of WT (D), *an3-4* (E), *KRP2* o/x (F) and *an3-4 KRP2* o/x (G) observed from a paradermal view. Cells of typical size for each genotype are outlined in red. (**H**) The first leaves of WT, *an3-4*, *KRP2* o/x and *an3-4 KRP2* o/x (left to right). Leaves of 21-day-old *Arabidopsis* plants were collected, fixed and cleared for observation. Scale bars: 50 μm in D; 5 mm in H.

accelerate the normal cell expansion pathway in which the *XS1*, *XS2*, *XS4* and *XS5* genes might be involved. Alternatively, one of them might encode factor X itself. The cloning of these genes and functional analyses are now in progress in our laboratory.

In contrast to *an3*-dependent compensation, we showed that compensation in *KRP2* o/x functions in a cell-autonomous manner. KRP2 is structurally and functionally related to KRP1, which has been shown to act non-cell-autonomously (De Veylder et al., 2001; Weinl et al., 2005). This suggests that native KRP2 might also inhibit cell proliferation non-cell-autonomously in leaf primordia. However, in our system, the overexpressed KRP2 was designed to be incapable of intercellular movement by tagging with 3xGFP, and this showed that the compensation was a cell-autonomous process. These facts indicate that a downstream pathway in the inhibition of cell cycle progression by KRP2 acts in a cell-autonomous manner.

Cells in *KRP2* o/x leaves are twice the size of those of the WT during the stage of cell proliferation (De Veylder et al., 2001; Ferjani et al., 2007). Therefore, cells overexpressing *KRP2* enter the postmitotic process with more cytoplasmic components than WT cells. The cell-autonomous action of compensation in *KRP2* o/x might be a result of abundant cytoplasm. Alternatively, it has been speculated that a defect in cell proliferation might be memorised in each cell. In fission yeast, circular ribosomal DNA accumulates in direct proportion to the number of cell divisions and causes ageing (Sinclair and Guarente, 1997). The mechanism that links cell proliferation and cell expansion in a single cell remains an enigmatic, but interesting, issue.

Our experimental systems involved overexpression of *KRP2*; therefore, the physiological significance of this effect should be carefully considered. In the present study, we demonstrated that induction of compensation requires the ectopic overexpression of *KRP2* during the stage of active cell proliferation. This indicates that compensation is caused by a defect in mitotic cell cycling. A recent study indicated that DELLA proteins are likely to suppress cell proliferation activity in early leaf development by promoting the expression of cyclin-dependent kinase inhibitor genes, including *KRP2* (Achard et al., 2009). Nevertheless, the accumulation of DELLA proteins suppresses postmitotic cell expansion without induction of compensation (Achard et al., 2009). Therefore, it would be worth considering the effect of *KRP2* overexpression in actively proliferating cells on the subsequent postmitotic cell expansion in which the DELLA factors are involved.

In summary, our studies show that during normal leaf development, cell proliferation is linked with postmitotic cell expansion in a cell-autonomous and a non-cell-autonomous manner. These findings should provide novel insight into the mechanism of organ size control in plants.

Acknowledgements

We thank Prof. T. Takahashi (Okayama University, Japan) and Dr H. Ichikawa (National Institute of Agrobiological Science, Japan) for providing seeds of the *HSP::Cre* lines and pSMAB704 binary vector, respectively. This work was supported by grants-in-aid for Creative Scientific Research (No. 18GS0313 to H.T.), Scientific Research on Priority Areas (No. 19060002 to H.T.), Scientific Research A (No. 17207005 to H.T. and G.H.), Exploratory Research (No.

18657020 to G.H.), a fellowship from the Japan Society for the Promotion of Science (JSPS) (No. 217214 to K.K.) and the Toray Science Foundation (to H.T.). This article is freely accessible online from the date of publication.

Competing interests statement
The authors declare no competing financial interests.

Supplementary material
Supplementary material for this article is available at
http://dev.biologists.org/lookup/suppl/doi:10.1242/dev.057117/-/DC1

References

Achard, P., Gusti, A., Cheminant, S., Alioua, M., Dhondt, S., Coppens, F., Beemster, G. T. and Genschik, P. (2009). Gibberellin signaling controls cell proliferation rate in Arabidopsis. *Curr. Biol.* **19**, 1188-1193.
Beemster, G. T., Fiorani, F. and Inzé, D. (2003). Cell cycle: the key to plant growth control? *Trends Plant Sci.* **8**, 154-158.
Clough, S. J. and Bent, A. F. (1998). Floral dip: a simplified method for Agrobacterium-mediated transformation of *Arabidopsis thaliana*. *Plant J.* **16**, 735-743.
De Veylder, L., Beeckman, T., Beemster, G. T., Krols, L., Terras, F., Landrieu, I., van der Schueren, E., Maes, S., Naudts, M. and Inzé, D. (2001). Functional analysis of cyclin-dependent kinase inhibitors of Arabidopsis. *Plant Cell* **13**, 1653-1668.
Donnelly, P. M., Bonetta, D., Tsukaya, H., Dengler, R. E. and Dengler, N. G. (1999). Cell cycling and cell enlargement in developing leaves of Arabidopsis. *Dev. Biol.* **215**, 407-419.
Ferjani, A., Horiguchi, G., Yano, S. and Tsukaya, H. (2007). Analysis of leaf development in *fugu* mutants of Arabidopsis reveals three compensation modes that modulate cell expansion in determinate organs. *Plant Physiol.* **144**, 988-999.
Fujikura, U., Horiguchi, G. and Tsukaya, H. (2007a). Dissection of enhanced cell expansion processes in leaves triggered by a defect in cell proliferation, with reference to roles of endoreduplication. *Plant Cell Physiol.* **48**, 278-286.
Fujikura, U., Horiguchi, G. and Tsukaya, H. (2007b). Genetic relationship between *angustifolia3* and *extra-small sisters* highlights novel mechanisms controlling leaf size. *Plant Signal. Behav.* **2**, 378-380.
Fujikura, U., Horiguchi, G., Ponce, M. R., Micol, J. L. and Tsukaya, H. (2009). Coordination of cell proliferation and cell expansion mediated by ribosome-related processes in the leaves of *Arabidopsis thaliana*. *Plant J.* **59**, 499-508.
Gamborg, O. L., Miller, R. A. and Ojima, K. (1968). Nutrient requirements of suspension cultures of soybean root cells. *Exp. Cell Res.* **50**, 151-158.
Haber, A. H. (1962). Nonessentiality of concurrent cell divisions for degree of polarization of leaf growth. I. Studies with radiation-induced mitotic inhibition. *Am. J. Bot.* **49**, 583-589.
Hemerly, A., Engler Jde, A., Bergounioux, C., Van Montagu, M., Engler, G., Inzé, D. and Ferreira, P. (1995). Dominant negative mutants of the Cdc2 kinase uncouple cell division from iterative plant development. *EMBO J.* **14**, 3925-3936.
Horiguchi, G., Kim, G. T. and Tsukaya, H. (2005). The transcription factor AtGRF5 and the transcription coactivator AN3 regulate cell proliferation in leaf primordia of *Arabidopsis thaliana*. *Plant J.* **43**, 68-78.
Horiguchi, G., Fujikura, U., Ferjani, A., Ishikawa, N. and Tsukaya, H. (2006). Large-scale histological analysis of leaf mutants using two simple leaf observation methods: identification of novel genetic pathways governing the size and shape of leaves. *Plant J.* **48**, 638-644.
Ichihashi, Y., Horiguchi, G., Gleissberg, S. and Tsukaya, H. (2010). The bHLH transcription factor *SPATULA* controls final leaf size in *Arabidopsis thaliana*. *Plant Cell Physiol.* **51**, 252-261.
Kazama, T., Ichihashi, Y., Murata, S. and Tsukaya, H. (2010). The mechanism of cell cycle arrest front progression explained by a *KLUH/CYP78A5*-dependent mobile growth factor in developing leaves of *Arabidopsis thaliana*. *Plant Cell Physiol.* **51**, 1046-1054.
Kim, J. H. and Kende, H. (2004). A transcriptional coactivator, AtGIF1, is involved in regulating leaf growth and morphology in Arabidopsis. *Proc. Natl. Acad. Sci. USA* **101**, 13374-13379.
Lui, H., Wang, H., Delong, C., Fowke, L. C., Crosby, W. L. and Fobert, P. R. (2000). The Arabidopsis Cdc2a-interacting protein ICK2 is structurally related to ICK1 and is a potent inhibitor of cyclin-dependent kinase activity in vitro. *Plant J.* **21**, 379-385.
Melaragno, J. E., Mehrotra, B. and Coleman, A. W. (1993). Relationship between endopolyploidy and cell size in epidermal tissue of Arabidopsis. *Plant Cell* **5**, 1661-1668.
Micol, J. L. (2009). Leaf development: time to turn over a new leaf? *Curr. Opin. Plant Biol.* **12**, 9-16.
Murashige, T. and Skoog, F. (1962). A revised medium for rapid growth and bio-assays with tobacco tissue cultures. *Physiol. Plant.* **15**, 473-497.
Nath, U., Crawford, B. C., Carpenter, R. and Coen, E. (2003). Genetic control of surface curvature. *Science* **299**, 1404-1407.
Ormenese, S., de Almeida Engler, J., De Groodt, R., De Veylder, L., Inzé, D. and Jacqmard, A. (2004). Analysis of the spatial expression pattern of seven Kip related proteins (KRPs) in the shoot apex of *Arabidopsis thaliana*. *Ann. Bot.* **93**, 575-580.
Serralbo, O., Perez-Perez, J. M., Heidstra, R. and Scheres, B. (2006). Non-cell-autonomous rescue of anaphase-promoting complex function revealed by mosaic analysis of HOBBIT, an Arabidopsis CDC27 homolog. *Proc. Natl. Acad. Sci. USA* **103**, 13250-13255.
Sieburth, L. E., Drews, G. N. and Meyerowitz, E. M. (1998). Non-autonomy of *AGAMOUS* function in flower development: use of a Cre/*loxP* method for mosaic analysis in *Arabidopsis*. *Development* **125**, 4303-4312.
Sinclair, D. A. and Guarente, L. (1997). Extrachromosomal rDNA circles-a cause of aging in yeast. *Cell* **91**, 1033-1042.
Takahashi, T. and Komeda, Y. (1989). Characterization of two genes encoding small heat-shock proteins in *Arabidopsis thaliana*. *Mol. Gen. Genet.* **219**, 365-372.
Tsukaya, H. (2002). Interpretation of mutants in leaf morphology: genetic evidence for a compensatory system in leaf morphogenesis that provides a new link between cell and organismal theories. *Int. Rev. Cytol.* **217**, 1-39.
Tsukaya, H. (2008). Controlling size in multicellular organs: focus on the leaf. *PLoS Biol.* **6**, 1373-1376.
Verkest, A., Manes, C. L., Vercruysse, S., Maes, S., Van Der Schueren, E., Beeckman, T., Genschik, P., Kuiper, M., Inzé, D. and De Veylder, L. (2005). The cyclin-dependent kinase inhibitor KRP2 controls the onset of the endoreduplication cycle during Arabidopsis leaf development through inhibition of mitotic CDKA;1 kinase complexes. *Plant Cell* **17**, 1723-1736.
Weinl, C., Marquardt, S., Kuijt, S. J., Nowack, M. K., Jakoby, M. J., Hulskamp, M. and Schnittger, A. (2005). Novel functions of plant cyclin-dependent kinase inhibitors, ICK1/KRP1, can act non-cell-autonomously and inhibit entry into mitosis. *Plant Cell* **17**, 1704-1722.
White, D. W. (2006). PEAPOD regulates lamina size and curvature in Arabidopsis. *Proc. Natl. Acad. Sci. USA* **103**, 13238-13243.